Published for SISSA by Springer
Received: December 1, 2013
Revised: March 1, 2014
Accepted: April 13, 2014
Published: April 30, 2014

Full one-loop electroweak corrections to $e^+e^- \to ZH\gamma$ at a Higgs factory

Ning Liu,[a,b] **Jie Ren,**[a,c] **Lei Wu,**[b] **Peiwen Wu**[c] **and Jin Min Yang**[c]

[a] *College of Physics and Electronic Engineering, Henan Normal University, Xinxiang 453007, China*
[b] *ARC Centre of Excellence for Particle Physics at the Terascale, School of Physics, The University of Sydney, NSW 2006, Australia*
[c] *State Key Laboratory of Theoretical Physics, Institute of Theoretical Physics, Academia Sinica, Beijing 100190, China*

E-mail: wlln@mail.ustc.edu.cn, jieren21@live.com, leiwu@physics.usyd.edu.au, pwwu@itp.ac.cn, jmyang@itp.ac.cn

Abstract: Motivated by the future precision test of the Higgs boson at an e^+e^- Higgs factory, we calculate the production $e^+e^- \to ZH\gamma$ in the Standard Model with complete next-to-leading order electroweak corrections. We find that for $\sqrt{s} = 240$ (350) GeV the cross section of this production is sizably reduced by the electroweak corrections, which is 1.03 (5.32) fb at leading order and 0.72 (4.79) fb at next-to-leading order. The transverse momentum distribution of the photon in the final states is also presented.

Keywords: NLO Computations

ArXiv ePrint: 1311.6971

doi:10.1007/JHEP04(2014)189

Contents

1 Introduction

Recently, a Standard Model (SM)-like Higgs boson around 125 GeV was observed by ATLAS and CMS collaborations at the LHC [1, 2]. This discovery is a great step towards the understanding of electroweak symmetry breaking of the SM. So far, most measurements of the properties of this new boson are consistent with the SM prediction. The new physics that affects the Higgs couplings has been cornered to a decoupling region [3, 4]. Besides, since many extensions of the SM (like the supersymmetric models) contain a SM-like Higgs boson [5–17] whose properties can be quite similar to the SM Higgs boson, it is difficult for the LHC to verify whether or not this new boson is the SM one. In order to precisely study this newly discovered Higgs boson, an e^+e^- collider, the so-called Higgs factory, is needed.

In such an e^+e^- Higgs factory, the properties of Higgs boson can be measured with rather high precisions [18–20]. The dominant Higgs production is the Higgs-strahlung process $e^+e^- \to ZH$, where the ZH events can be inclusively detected by tagging a leptonic Z decay without the assumption of the Higgs decay mode. The individual Higgs decay branching ratios can then be directly measured as the fractions of the total $e^+e^- \to ZH$ cross section by observing the specific states. For $\sqrt{s} \sim 240 - 250\,\text{GeV}$ with an integrated luminosity of $500\,\text{fb}^{-1}$, about $O(10^5)$ Higgs bosons can be produced per year, which allows to measure the Higgs couplings at a few percent [20]. So the electroweak radiative corrections should be taken into account in the theoretical calculations of the production rate. For the process $e^+e^- \to ZH$, the leading order calculation was performed in [21] and the one-loop electroweak corrections were calculated with the soft-photon approximation in [22–24] (a compact analytical formula for the electromagnetic corrections was given in [23] and a numerical calculation algorithm for the real photon emission was proposed in [25]).

For an e^+e^- Higgs factory with $\sqrt{s} \sim 240 - 250\,\text{GeV}$ another possibly important process is $e^+e^- \to HZ\gamma$. On one hand, it is an important part of the inclusive process $e^+e^- \to ZH + X$ or can be distinguished for a hard photon; On the other hand, since the $HZ\gamma$ vertex occurs at one loop in the SM, the $HZ\gamma$ couplings is particularly sensitive to possible new physics contributions, such as the existence of new heavy particles propagating in the loop [26, 27]. In this work we calculate this production in the SM with the complete

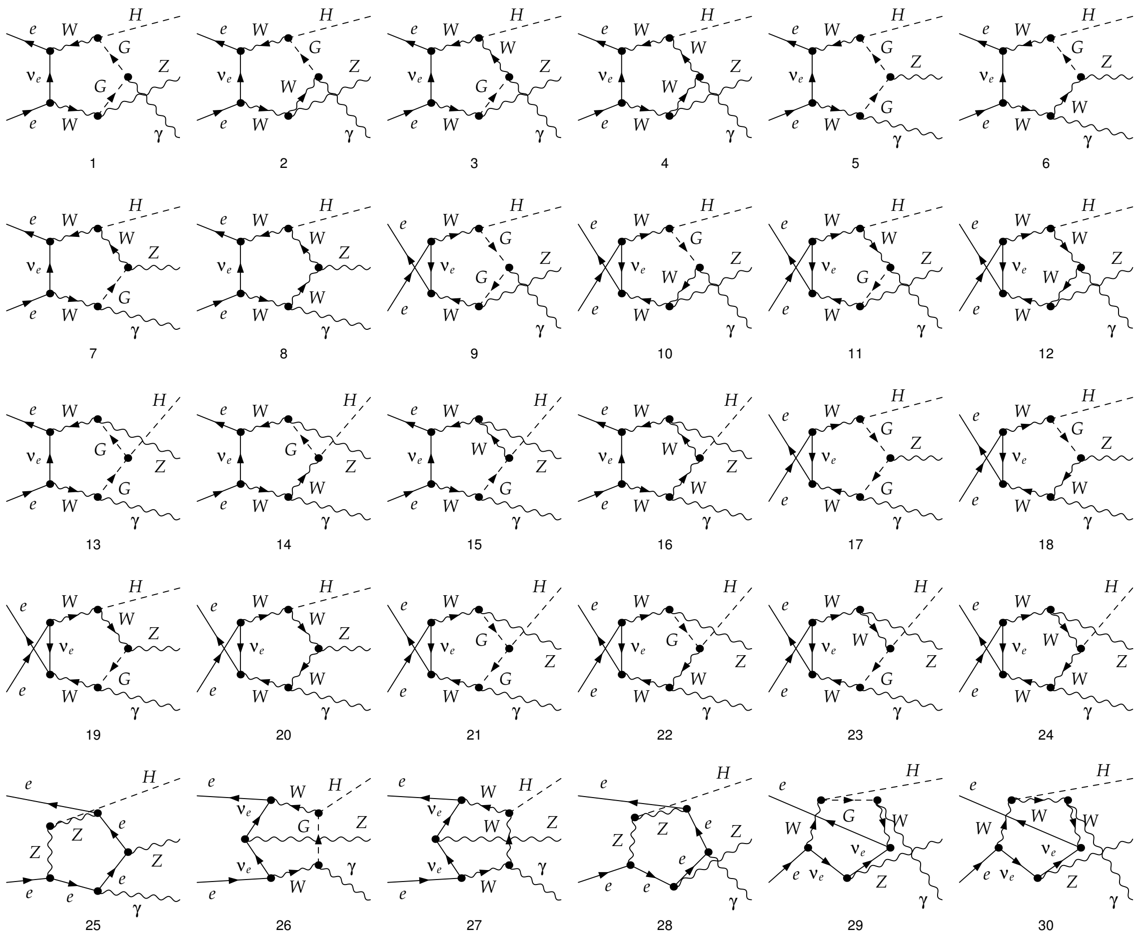

Figure 1. The pentagon diagrams for the process $e^+e^- \to HZ\gamma$.

next-to-leading order electroweak (NLO EW) corrections. In section II we will give a description for the analytic calculations. The numerical results and discussions are given in section III. Finally, we draw our conclusions in section IV.

2 A description of analytical calculations

In the SM the process $e^+e^- \to HZ\gamma$ is induced by the electroweak interaction at leading order (LO). Due to the small Yukawa couplings, we ignore the contributions from the Feynman diagrams involving the Yukawa couplings of light fermions. We denote the four-momenta of initial and final states in the process as

$$e^+(q_1) + e^-(q_2) \to H(q_3) + Z(q_4) + \gamma(q_5) \tag{2.1}$$

The NLO EW corrections ($\Delta\sigma_{EW}$) include two parts:

- Virtual correction ($\Delta\sigma_{vir}$).
  We adopt the dimensional regularization to isolate the ultraviolet divergences (UV)

in the one-loop amplitudes. Then we remove the UV singularities by using the on-mass-shell renormalization scheme [28–30]. The pentagon Feynman diagrams in the calculation are presented in figure 1. The reductions of N-point ($N \leq 4$) tensor integrals are implemented by using the Passarino-Veltman algorithm [31, 32]. But for the calculation of the 5-point tensor functions, we adopt the Denner-Dittmaier method developed in ref. [33] to reduce the tensor integrals and use our fortran subroutines to perform numerical study, which has been validated in our previous works [34, 35]. We also numerically checked that our results are UV finite.

- Real photon radiation ($\Delta\sigma_{real}$).
Due to the exchange of virtual photon in the loops, the infrared (IR) divergences can appear in the virtual correction. According to the Kinoshita-Lee-Nauenberg (KLN) theorem [36, 37], these IR divergences will be canceled by the real photon bremsstrahlung corrections in the soft photon limit. We denote the momenta of initial and final states for the real photon radiation process as

$$e^+(q_1) + e^-(q_2) \to H(q_3) + Z(q_4) + \gamma(q_5) + \gamma(q_6). \tag{2.2}$$

We take the phase-space-slicing method [38–41] to isolate the IR singularity in the above process. An arbitrarily small cut-off parameter δ_s is introduced to split the phase space into soft region ($E_6 \leq \delta_s\sqrt{s}/2$) and hard region ($E_6 > \delta_s\sqrt{s}/2$). So the real photon emission correction can be decomposed into the soft and hard parts:

$$\Delta\sigma_{real} = \Delta\sigma_{soft} + \Delta\sigma_{hard}. \tag{2.3}$$

In the soft photon approximation [42], we can calculate the soft part of the correction by using the following equation

$$d\Delta\sigma_{soft} = d\sigma_0 \frac{\alpha}{2\pi^2} \int_{E_6 \leq \delta_s\sqrt{s}/2} \frac{d^3\vec{q}_6}{2E_6} \left(\frac{q_1}{q_1 \cdot q_6} - \frac{q_2}{q_2 \cdot q_6} \right)^2 . \tag{2.4}$$

where $E_6 = \sqrt{|\vec{q}_6|^2 + m_\gamma^2}$ and we give a small mass m_γ to the photon to eliminate the IR divergence (we checked that the dependence on this non-physical mass m_γ is exactly canceled when the real radiation correction and the virtual correction are combined). Since the hard part of the correction is insensitive to this fictitious photon mass, it can be directly evaluated by the numerical Monte Carlo method [43]. We notice that there are two photons in the real emission process and one of them should be tagged as the observed hard photon with $p_T > 10\,\mathrm{GeV}$ and $|\eta| < 2$. The phase space integral of these two identical photons in hard part of real emission can be expressed as:

$$\begin{aligned} I_{56} \sim \frac{1}{2} \Bigg[&\int_{E_c}^{\infty} \frac{d^3\vec{q}_5}{2E_5} \int_{\delta_s\sqrt{s}/2}^{E_5} \frac{d^3\vec{q}_6}{2E_6} |\mathcal{M}|^2 \theta(E_5 - E_6) \\ &+ \int_{E_c}^{\infty} \frac{d^3\vec{q}_6}{2E_6} \int_{\delta_s\sqrt{s}/2}^{E_6} \frac{d^3\vec{q}_5}{2E_5} |\mathcal{M}|^2 \theta(E_6 - E_5) \Bigg] , \end{aligned} \tag{2.5}$$

$\sqrt{s}$	$\sigma_{LO}^{F.G.}$ (our)	$\sigma_{LO}^{U.G.}$ (CompHEP)
250	2.172(2)	2.172(4)
350	5.316(5)	5.316(9)
500	3.562(3)	3.561(6)
600	2.705(3)	2.705(4)
800	1.708(2)	1.708(3)
1000	1.184(1)	1.184(2)

Table 1. The comparison of our LO cross section of $e^+e^- \to HZ\gamma$ in Feynman gauge with those calculated by CompHEP 4.5.2 in unitary gauge.

where the factor $\frac{1}{2}$ is from the identical photons in the final states, and E_c is the energy cut that corresponds to the above hard p_T cut. In order to improve the numerical stability of eq. (2.5), we adopt the method in the ref. [44] to carry out the integral eq. (2.5). Since each of the two photons in the final states can be softer or harder than the other one with an equal probability, the eq. (2.5) can be equivalent to:

$$I_{56} \sim \frac{1}{2} \times 2 \times \int_{E_c}^{\infty} \frac{d^3\vec{q}_5}{2E_5} \int_{\delta_s\sqrt{s}/2}^{E_5} \frac{d^3\vec{q}_6}{2E_6} |\mathcal{M}|^2. \tag{2.6}$$

This means that we can technically assume the photon $\gamma(q_5)$ to be the tagged hard photon and impose a transverse momentum cut $p_T > 10\,\text{GeV}$ and pseudo-rapidity cut $|\eta| < 2$ on $\gamma(q_5)$ in the numerical calculations [44, 45].

Finally, the total NLO EW correction of the process $e^+e^- \to HZ\gamma$ is obtained by

$$\Delta\sigma_{\text{tot}} = \Delta\sigma_{vir} + \Delta\sigma_{soft} + \Delta\sigma_{hard}. \tag{2.7}$$

We do the calculations by using the packages FeynArts-3.8 [46], FormCalc-8.2 [47] and LoopTools-2.8 [48–50] (we have the experience for using such packages [34, 35, 51, 52]). We analytically checked the gauge independence of our LO result by using the Ward identities. We also numerically checked our LO calculations in Feynman gauge(F.G.) with the package CompHEP 4.5.2 in unitary gauge(U.G.) [53]. In tableI, we present the comparison results and find that they are well consistent and are gauge-independent. In addition, by simultaneously interchanging the momenta and the polarization vectors of the two photons, we exploit Bose symmetry of the amplitudes of the real emission processes and found the values of the corresponding amplitudes do not change within numerical precision. We also numerically checked our result for the real radiation correction by using the Comphep program and found good agreement.

3 Numerical results and discussions

In the numerical calculations we take the input parameters of the SM as [54]

$$\begin{aligned} m_t = 171.2 \text{ GeV}, \quad m_e = 0.519991 \text{ MeV}, \quad m_Z = 91.19 \text{ GeV}, \\ \sin^2\theta_W = 0.2228, \quad \alpha(m_Z^2)^{-1} = 127.918. \end{aligned} \tag{3.1}$$

JHEP04(2014)189

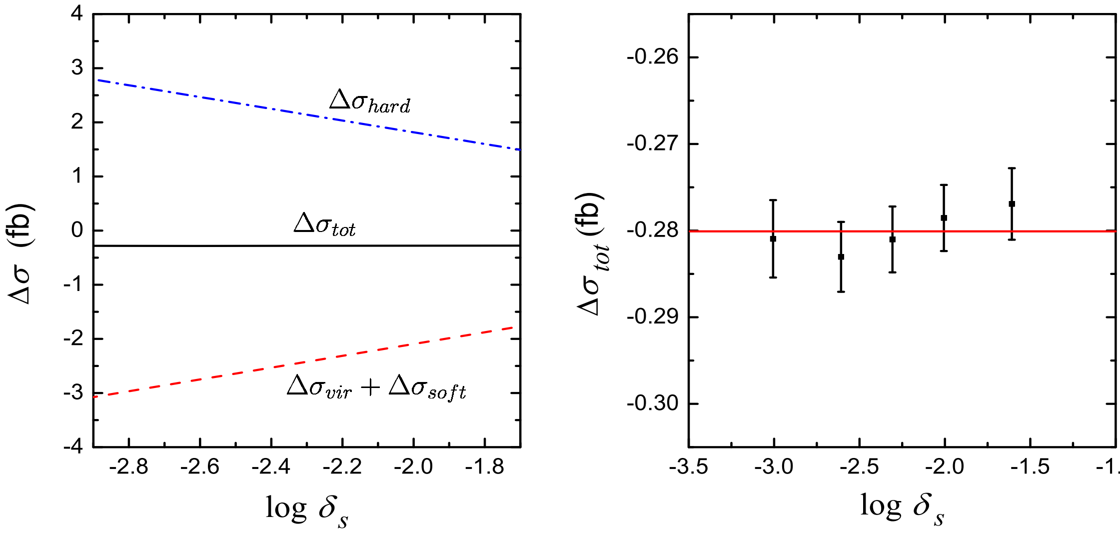

Figure 2. The one-loop electroweak correction to the cross section of $e^+e^- \to HZ\gamma$ versus the soft cutoff $\log\delta_s$ for $M_H = 125.66\,\mathrm{GeV}$ and $\sqrt{s} = 500\,\mathrm{GeV}$: (a) showing respectively $\Delta\sigma_{hard}$, $\Delta\sigma_{vir} + \Delta\sigma_{soft}$ and $\Delta\sigma_{\rm tot}$; (b) showing $\Delta\sigma_{\rm tot}$ with the calculation errors.

The Higgs mass is taken as $m_H = 125.66 \pm 0.34\,\mathrm{GeV}$ [4], which is the combined result of the measurements of the ATLAS and CMS collaborations.

We numerically check the stability of the results versus the soft photon cutoff parameter in figure 2, where we assume $\sqrt{s} = 500\,\mathrm{GeV}$ and $m_\gamma = 10^{-8}$ GeV. From the left panel of figure 2 it can be seen that the values of $\Delta\sigma_{vir}$, $\Delta\sigma_{hard}$ and $\Delta\sigma_{soft}$ depend on the soft cutoff $\log\delta_s$, while the total NLO EW correction $\Delta\sigma_{\rm tot}$ is independent of $\log\delta_s$ within reasonable calculation errors. Besides, we checked that the total correction is independent of m_γ for a fixed δ_s. Therefore, in the following calculations we take the $\delta_s = 2\times 10^{-3}$ and $m_\gamma = 10^{-8}$ GeV.

In figure 3 we plot the cross section of $e^+e^- \to HZ\gamma$ versus the center-of-mass energy $\sqrt{s}$, showing respectively the LO result and the NLO EW corrections. We can see that the production rate can reach a few fb in the threshold region $\sqrt{s} \sim 300 - 350$ GeV (maximally it can reach 5.5 fb at LO and 4.8 fb at NLO), and the corresponding EW correction can reach -12%. For $\sqrt{s} > 400$ GeV, the cross section decreases rapidly due to the suppression of $1/s$. At a 240 GeV Higgs factory, like the proposed LEP3 or China Higgs Factory (CHF), the cross section of $e^+e^- \to HZ\gamma$ can reach 1.03 fb at LO and 0.72 fb at NLO (the corresponding EW correction is -30%), while at a 350 GeV Higgs factory, such as the ILC and TLEP, the cross section of $e^+e^- \to HZ\gamma$ will reach 5.32 fb at LO and 4.79 fb at NLO (the corresponding EW correction is -9.8%). We can also find that the uncertainty of the cross section caused by the Higgs mass becomes small with the increase of $\sqrt{s}$.

Finally in figure 4 we show the transverse momentum distribution of the photon in the process $e^+e^- \to HZ\gamma$ at LO and NLO for $\sqrt{s} = 240, 350$ GeV. It can be seen that the NLO EW correction can greatly reduce the LO differential cross section at low p_T region. The impact of the uncertainty of the Higgs mass on the p_T distribution becomes weak as the collider energy increases. For $\sqrt{s} = 240\,\mathrm{GeV}$ most of the events are produced in the

JHEP04(2014)189

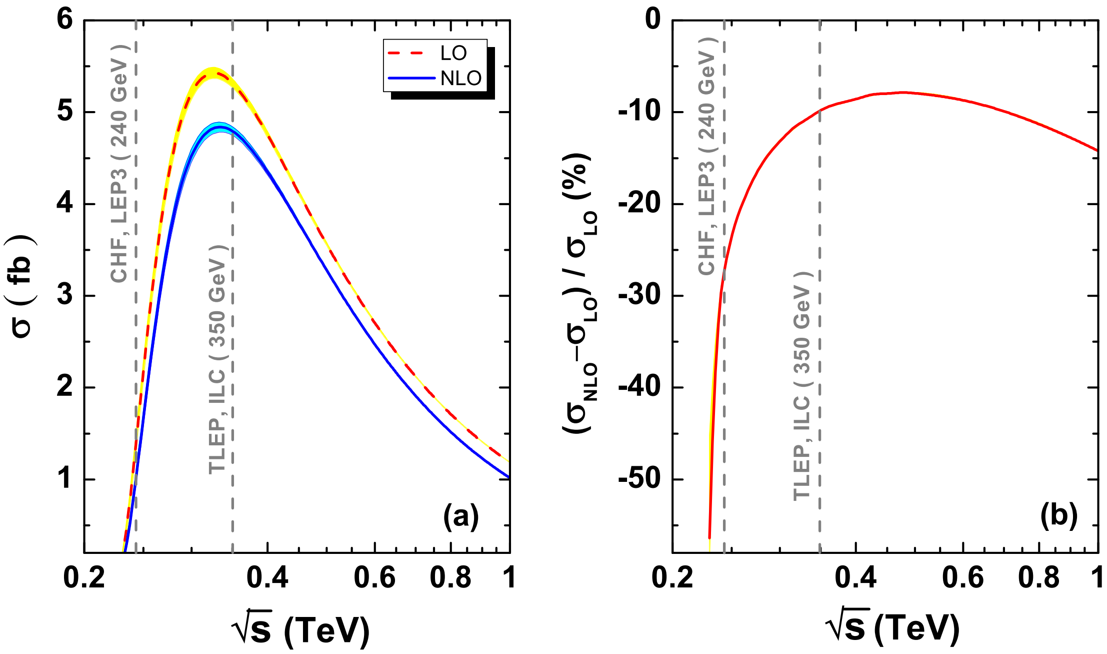

Figure 3. The cross section of $e^+e^- \to HZ\gamma$ versus $\sqrt{s}$, showing respectively the LO result and the NLO EW corrections. The uncertainty caused by the 2σ range of the Higgs mass (124.98 GeV $< m_H <$ 126.44 GeV) is also shown (the shaded bands).

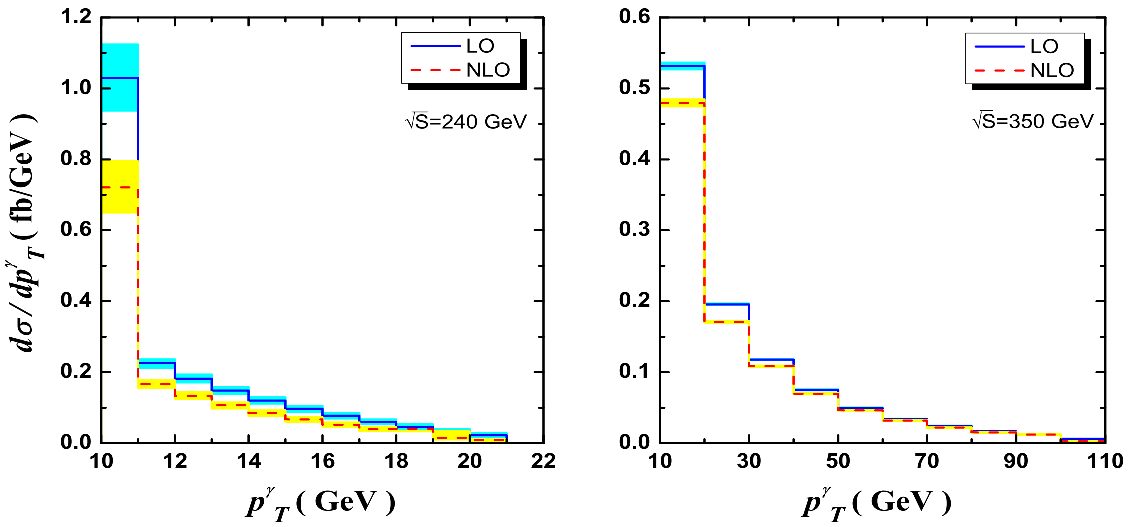

Figure 4. The transverse momentum distribution of the photon at LO and NLO for the process $e^+e^- \to HZ\gamma$ with $\sqrt{s} = 240, 350\,\text{GeV}$. The shaded bands correspond to the uncertainty caused by the 2σ range of the Higgs mass (124.98 GeV $< m_H <$ 126.44 GeV).

region of $p_T^\gamma < 20$ GeV due to the center-of-mass energy close to the production threshold; while for $\sqrt{s} = 350\,\text{GeV}$ the p_T value of the photon gets much harder.

4 Conclusion

In this work we calculated the cross section of $e^+e^- \to ZH\gamma$ with complete next-to-leading order electroweak corrections in the SM. We found that for $\sqrt{s} = 240$ (350) GeV the cross section of this production can reach 1.03 (5.32) fb at leading order and 0.72 (4.79) fb at next-to-leading order. In a future e^+e^- Higgs factory, this process can be measured as a precision test of the SM.

Acknowledgments

We appreciate the helpful discussion with Chengcheng Han. Ning Liu would like to thank Dr Archil Kobakhidze for his warm hospitality in Sydney node of CoEPP in Australia. This work is supported by the National Natural Science Foundation of China (NNSFC) under grant Nos.11305049, 11275057, 11275245, 10821504 and 11135003, by Specialized Research Fund for the Doctoral Program of Higher Education under Grant No.20134104120002, and by the Startup Foundation for Doctors of Henan Normal University under contract No.11112.

References

[1] ATLAS collaboration, *Observation of a new particle in the search for the Standard Model Higgs boson with the ATLAS detector at the LHC*, Phys. Lett. **B 716** (2012) 1 [arXiv:1207.7214] [INSPIRE].

[2] CMS collaboration, *Observation of a new boson at a mass of 125 GeV with the CMS experiment at the LHC*, Phys. Lett. **B 716** (2012) 30 [arXiv:1207.7235] [INSPIRE].

[3] G. Bélanger, B. Dumont, U. Ellwanger, J.F. Gunion and S. Kraml, *Global fit to Higgs signal strengths and couplings and implications for extended Higgs sectors*, Phys. Rev. **D 88** (2013) 075008 [arXiv:1306.2941] [INSPIRE].

[4] P.P. Giardino, K. Kannike, I. Masina, M. Raidal and A. Strumia, *The universal Higgs fit*, arXiv:1303.3570 [INSPIRE].

[5] M. Carena, S. Gori, N.R. Shah and C.E.M. Wagner, *A 125 GeV SM-like Higgs in the MSSM and the $\gamma\gamma$ rate*, JHEP **03** (2012) 014 [arXiv:1112.3336] [INSPIRE].

[6] M. Carena, S. Gori, N.R. Shah, C.E.M. Wagner and L.-T. Wang, *Light Stau Phenomenology and the Higgs $\gamma\gamma$ Rate*, JHEP **07** (2012) 175 [arXiv:1205.5842] [INSPIRE].

[7] J. Cao, Z. Heng, J.M. Yang and J. Zhu, *Status of low energy SUSY models confronted with the LHC 125 GeV Higgs data*, JHEP **10** (2012) 079 [arXiv:1207.3698] [INSPIRE].

[8] J.-J. Cao, Z.-X. Heng, J.M. Yang, Y.-M. Zhang and J.-Y. Zhu, *A SM-like Higgs near 125 GeV in low energy SUSY: a comparative study for MSSM and NMSSM*, JHEP **03** (2012) 086 [arXiv:1202.5821] [INSPIRE].

[9] J. Cao, Z. Heng, D. Li and J.M. Yang, *Current experimental constraints on the lightest Higgs boson mass in the constrained MSSM*, Phys. Lett. **B 710** (2012) 665 [arXiv:1112.4391] [INSPIRE].

[10] U. Ellwanger, *A Higgs boson near 125 GeV with enhanced di-photon signal in the NMSSM*, JHEP **03** (2012) 044 [arXiv:1112.3548] [INSPIRE].

[11] G. Bélanger et al., *Higgs Bosons at 98 and 125 GeV at LEP and the LHC*, JHEP **01** (2013) 069 [arXiv:1210.1976] [INSPIRE].

[12] G. Bélanger, U. Ellwanger, J.F. Gunion, Y. Jiang and S. Kraml, *Two Higgs Bosons at the Tevatron and the LHC?*, arXiv:1208.4952 [INSPIRE].

[13] J.F. Gunion, Y. Jiang and S. Kraml, *Could two NMSSM Higgs bosons be present near 125 GeV?*, Phys. Rev. **D 86** (2012) 071702 [arXiv:1207.1545] [INSPIRE].

[14] J.F. Gunion, Y. Jiang and S. Kraml, *Diagnosing Degenerate Higgs Bosons at 125 GeV*, Phys. Rev. Lett. **110** (2013) 051801 [arXiv:1208.1817] [INSPIRE].

[15] J. Cao, C. Han, L. Wu, J.M. Yang and Y. Zhang, *Probing Natural SUSY from Stop Pair Production at the LHC*, JHEP **11** (2012) 039 [arXiv:1206.3865] [INSPIRE].

[16] C. Han et al., *Probing Light Higgsinos in Natural SUSY from Monojet Signals at the LHC*, JHEP **02** (2014) 049 [arXiv:1310.4274] [INSPIRE].

[17] C. Han, K.-i. Hikasa, L. Wu, J.M. Yang and Y. Zhang, *Current experimental bounds on stop mass in natural SUSY*, JHEP **10** (2013) 216 [arXiv:1308.5307] [INSPIRE].

[18] A. Blondel et al., *Report of the ICFA Beam Dynamics Workshop 'Accelerators for a Higgs Factory: Linear vs. Circular' (HF2012)*, arXiv:1302.3318 [INSPIRE].

[19] S. Dawson et al., *Higgs Working Group Report of the Snowmass 2013 Community Planning Study*, arXiv:1310.8361 [INSPIRE].

[20] M.E. Peskin, *Comparison of LHC and ILC Capabilities for Higgs Boson Coupling Measurements*, arXiv:1207.2516 [INSPIRE].

[21] J.R. Ellis, M.K. Gaillard and D.V. Nanopoulos, *A Phenomenological Profile of the Higgs Boson*, Nucl. Phys. **B 106** (1976) 292 [INSPIRE].

[22] J. Fleischer and F. Jegerlehner, *Radiative Corrections to Higgs Production by $e^+e^- \to ZH$ in the Weinberg-Salam Model*, Nucl. Phys. **B 216** (1983) 469 [INSPIRE].

[23] B.A. Kniehl, *Radiative corrections for associated ZH production at future e^+e^- colliders*, Z. Phys. **C 55** (1992) 605 [INSPIRE].

[24] A. Denner, J. Kublbeck, R. Mertig and M. Böhm, *Electroweak radiative corrections to $e^+e^- \to HZ$*, Z. Phys. **C 56** (1992) 261 [INSPIRE].

[25] F.A. Berends and R. Kleiss, *Initial State Radiation at LEP Energies and the Corrections to Higgs Boson Production*, Nucl. Phys. **B 260** (1985) 32 [INSPIRE].

[26] J. Cao, L. Wu, P. Wu and J.M. Yang, *The Z+photon and diphoton decays of the Higgs boson as a joint probe of low energy SUSY models*, JHEP **09** (2013) 043 [arXiv:1301.4641] [INSPIRE].

[27] C. Han, N. Liu, L. Wu, J.M. Yang and Y. Zhang, *Two-Higgs-doublet model with a color-triplet scalar: a joint explanation for top quark forward-backward asymmetry and Higgs decay to diphoton*, Eur. Phys. J. **C 73** (2013) 2664 [arXiv:1212.6728] [INSPIRE].

JHEP04(2014)189

[28] M. Böhm, H. Spiesberger and W. Hollik, *On the One Loop Renormalization of the Electroweak Standard Model and Its Application to Leptonic Processes*, *Fortsch. Phys.* **34** (1986) 687 [INSPIRE].

[29] W.F.L. Hollik, *Radiative Corrections in the Standard Model and their Role for Precision Tests of the Electroweak Theory*, *Fortsch. Phys.* **38** (1990) 165 [INSPIRE].

[30] B. Grzadkowski and W. Hollik, *Radiative corrections to the top quark width within two Higgs doublet models*, *Nucl. Phys.* **B 384** (1992) 101 [INSPIRE].

[31] G. 't Hooft and M.J.G. Veltman, *Scalar One Loop Integrals*, *Nucl. Phys.* **B 153** (1979) 365 [INSPIRE].

[32] A. Denner, *Techniques for calculation of electroweak radiative corrections at the one loop level and results for W physics at LEP-200*, *Fortsch. Phys.* **41** (1993) 307 [arXiv:0709.1075] [INSPIRE].

[33] A. Denner and S. Dittmaier, *Reduction of one loop tensor five point integrals*, *Nucl. Phys.* **B 658** (2003) 175 [hep-ph/0212259] [INSPIRE].

[34] N. Liu, L. Wu, P.W. Wu and J.M. Yang, *Complete one-loop effects of SUSY QCD in $b\bar{b}h$ production at the LHC under current experimental constraints*, *JHEP* **01** (2013) 161 [arXiv:1208.3413] [INSPIRE].

[35] N. Liu, L. Guo, W.-G. Ma, R.-Y. Zhang and L. Han, *Supersymmetric QCD and CP-violation effects in $t\bar{t}Z^0$ production at the LHC*, *Phys. Rev.* **D 82** (2010) 015009 [INSPIRE].

[36] T. Kinoshita, *Mass singularities of Feynman amplitudes*, *J. Math. Phys.* **3** (1962) 650 [INSPIRE].

[37] CDF collaboration, T. Aaltonen et al., *Measurement of correlated $b^-\bar{b}$ production in $p^-\bar{p}$ collisions at $\sqrt{s} = 1960$ GeV*, *Phys. Rev.* **D 77** (2008) 072004 [arXiv:0710.1895] [INSPIRE].

[38] B.W. Harris and J.F. Owens, *The Two cutoff phase space slicing method*, *Phys. Rev.* **D 65** (2002) 094032 [hep-ph/0102128] [INSPIRE].

[39] W.T. Giele and E.W.N. Glover, *Higher order corrections to jet cross-sections in e^+e^- annihilation*, *Phys. Rev.* **D 46** (1992) 1980 [INSPIRE].

[40] W.T. Giele, E.W.N. Glover and D.A. Kosower, *Higher order corrections to jet cross-sections in hadron colliders*, *Nucl. Phys.* **B 403** (1993) 633 [hep-ph/9302225] [INSPIRE].

[41] S. Keller and E. Laenen, *Next-to-leading order cross-sections for tagged reactions*, *Phys. Rev.* **D 59** (1999) 114004 [hep-ph/9812415] [INSPIRE].

[42] S. Dawson and L. Reina, *QCD corrections to associated Higgs boson heavy quark production*, *Phys. Rev.* **D 59** (1999) 054012 [hep-ph/9808443] [INSPIRE].

[43] G.P. Lepage, *A New Algorithm for Adaptive Multidimensional Integration*, *J. Comput. Phys.* **27** (1978) 192 [INSPIRE].

[44] P.H. Khiem et al., *Full $\mathcal{O}(\alpha)$ electroweak radiative corrections to $e^+e^- \to t\bar{t}\gamma$ with GRACE-Loop*, *Eur. Phys. J.* **C 73** (2013) 2400 [arXiv:1211.1112] [INSPIRE].

[45] W. Hollik and C. Meier, *Electroweak corrections to γZ production at hadron colliders*, *Phys. Lett.* **B 590** (2004) 69 [hep-ph/0402281] [INSPIRE].

[46] T. Hahn, *Generating Feynman diagrams and amplitudes with FeynArts 3*, *Comput. Phys. Commun.* **140** (2001) 418 [hep-ph/0012260] [INSPIRE].

JHEP04(2014)189

[47] T. Hahn and M. Pérez-Victoria, *Automatized one loop calculations in four-dimensions and D-dimensions*, Comput. Phys. Commun. **118** (1999) 153 [hep-ph/9807565] [INSPIRE].

[48] G.J. van Oldenborgh, *FF: A Package to evaluate one loop Feynman diagrams*, *Phys Commun.* **66** (1991) 1 [NIKHEF-H-90].

[49] G. 't Hooft and M.J.G. Veltman, *Scalar One Loop Integrals*, Nucl. Phys. **B 153** (1979) 365 [INSPIRE].

[50] A. Denner, *Techniques for calculation of electroweak radiative corrections at the one loop level and results for W physics at LEP-200*, Fortsch. Phys. **41** (1993) 307 [arXiv:0709.1075] [INSPIRE].

[51] N. Liu, *QCD corrections to the production of $t\bar{t}\gamma$ at the ILC*, Phys. Lett. **B 707** (2012) 137 [arXiv:1112.3702] [INSPIRE].

[52] N. Liu, J. Ren and B. Yang, *Next-to-leading order QCD corrections to $HZW^{\pm}$ production at 14 TeV LHC*, Phys. Lett. **B 731** (2014) 70 [arXiv:1310.6192] [INSPIRE].

[53] A. Pukhov et al., *CompHEP: A Package for evaluation of Feynman diagrams and integration over multiparticle phase space*, hep-ph/9908288 [INSPIRE].

[54] Particle Data Group collaboration, J. Beringer et al., *Review of Particle Physics (RPP)*, Phys. Rev. **D 86** (2012) 010001 [INSPIRE].

JHEP04(2014)189